JOURNAL OF GEOPHYSICAL RESEARCH, VOL. 112, C06025, doi:10.1029/2006JC003886, 2007

Observations of the summer Red Sea circulation

Sarantis S. Sofianos[1] and William E. Johns[2]

Received 16 August 2006; revised 27 December 2006; accepted 2 April 2007; published 30 June 2007.

[1] Aiming at exploring and understanding the summer circulation in the Red Sea, a cruise was conducted in the basin during the summer of 2001 involving hydrographic, meteorological, and direct current observations. The most prominent feature, characteristic of the summer circulation and exchange with the Indian Ocean, is a temperature, salinity, and oxygen minimum located around a depth of 75 m at the southern end of the basin, associated with Gulf of Aden Intermediate Water inflowing from the Gulf of Aden during the summer season as an intruding subsurface layer. Stirring and mixing with ambient waters lead to marked increases in temperature (from 16.5 to almost 33°C) and salinity (from 35.7 to more than 38 psu) in this layer by the time it reaches midbasin. The observed circulation presents a very vigorous pattern with strong variability and intense features that extend the width of the basin. A permanent cyclone, detected in the northern Red Sea, verifies previous observations and modeling studies, while in the central sector of the basin a series of very strong anticyclones were observed with maximum velocities exceeding 1 m/s. The three-layer flow pattern, representative of the summer exchange between the Red Sea and the Gulf of Aden, is observed in the strait of Bab el Mandeb. In the southern part of the basin the layer flow is characterized by strong banking of the inflows and outflows against the coasts. Both surface and intermediate water masses involved in the summer Red Sea circulation present prominent spatial variability in their characteristics, indicating that the eddy field and mixing processes play an important role in the summer Red Sea circulation.

Citation: Sofianos, S. S., and W. E. Johns (2007), Observations of the summer Red Sea circulation, *J. Geophys. Res.*, *112*, C06025, doi:10.1029/2006JC003886.

1. Introduction

[2] From an oceanographic perspective the Red Sea is a very advantageous experimental basin with unique characteristics. It has a relatively simple shape and moderate size (4.5×10^6 km^3; about one fifth of the Mediterranean Sea), and the connection between the basin and the open ocean, the strait of Bab el Mandeb, is a very narrow and shallow channel (sill depth 160 m and narrowest point 25 km wide). The dynamics governing a large area are therefore reflected on a very small strait cross section of about 2 km^2. The Red Sea experiences strong seasonal atmospheric forcing through both wind stress and air-sea buoyancy fluxes. As a result of the very high evaporation rate which exceeds 2 m/yr [*Sofianos et al.*, 2002], the Red Sea produces one of the most saline water masses observed in the world ocean, the Red Sea Outflow Water (RSOW), which outflows from the basin and spreads into the Indian Ocean influencing the stratification over an extensive area.

[3] Despite its ecological importance, the Red Sea remains widely unexplored and several processes, including the basic circulation pattern and the water mass formation, are still obscure and highly debated. The very few expeditions carried out in the region were limited in spatial coverage [*Vercelli*, 1931; *Thompson*, 1939a, 1939b; *Siedler*, 1968; *Morcos*, 1970; *Morcos and Soliman*, 1974; *Maillard*, 1974; *Maillard and Soliman*, 1986; *Murray and Johns*, 1997] or followed the main axis of the basin [*Quadfasel and Baunder*, 1993]. Most of the available observations have been collected during the winter season, when a relatively simple two-layer exchange pattern is present in the southern part of the basin. On the basis of this kind of information, very few circulation features were identified and the general circulation pattern was often treated in a two-dimensional framework. The only exceptions are in the northernmost part of the basin where a general cyclonic circulation was observed through hydrographic observations [*Morcos*, 1970; *Morcos and Soliman*, 1974; *Maillard*, 1974] and verified by a limited set of drifter tracks during 1993–1994 [*Clifford et al.*, 1997], and the area of Bab el Mandeb where several observational efforts were carried out during the last century [*Vercelli*, 1927; *Siedler*, 1968; *Maillard and Soliman*, 1986; *Murray and Johns*, 1997].

[4] The most recent, long-term and comprehensive observations in the strait of Bab el Mandeb were carried out during 1995–1996 [*Murray and Johns*, 1997], lasting 18 months and monitoring velocity, temperature and salinity structure at the strait over the whole seasonal cycle. They

[1]Division of Applied Physics, University of Athens, Athens, Greece.
[2]Division of Meteorology and Physical Oceanography, Rosenstiel School of Marine and Atmospheric Sciences, University of Miami, Miami, Florida, USA.

0148-0227/07/2006JC003886$09.00

have greatly improved our picture of several aspects of the regional dynamics and at the same time have provided a starting point for investigating the circulation and water mass formation in the region and their variability in more detail. *Murray and Johns* [1997] confirmed most of the earlier deductions on the seasonal cycle of the exchange flow and showed that the transition between the typical inverse-estuarine two-layer winter exchange to a three-layer exchange pattern in summer is a robust feature of the seasonal flow pattern. The new data also made it possible to quantify the mean and seasonal exchange rates of the different water masses. The annual mean RSOW outflow, which is a good measure of the overall strength of the exchange, was estimated at 0.36 Sv but showed a large annual cycle ranging from over 0.6 Sv during winter (February) to less than 0.1 Sv during summer (August). The reversal of the surface flow and the intrusion of Gulf of Aden Intermediate Water (GAIW) lasts for four months (June to September) when an average of 0.22 Sv of GAIW enters the Red Sea.

[5] On the basis of the direct oceanographic observations at Bab el Mandeb, the annual mean heat and freshwater fluxes over the Red Sea were estimated to be 11 ± 5 W m^{-2} and 2.06 ± 0.22 m yr^{-1}, respectively [*Sofianos et al.*, 2002]. Using a consistent climatology of the air-sea fluxes, the mechanisms involved in the seasonal exchange flow at Bab el Mandeb were studied using the Miami Isopycnic Coordinate Ocean Model [*Sofianos and Johns*, 2002]. The model experiments were able to reproduce the basic characteristics of the observed seasonal exchange flow at strait and showed that the combined action of seasonal wind stress and thermohaline forcing can reproduce the seasonal variability of the circulation in the strait. Contrary to earlier ideas about a two-dimensional and sluggish Red Sea circulation, the model results presented a very active and complex circulation pattern, including intensification of the along-basin flow toward the coasts and a series of strong seasonal or permanent eddy-like features [*Sofianos and Johns*, 2003]. In the northern part of the basin, the results showed the presence of two permanent gyres, a cyclonic gyre in the northern end and a smaller anticyclonic gyre centered on 23.5°N. Their maximum velocities exceeded 40 cm/s and they penetrated the surface and intermediate layers. Strong seasonal eddy-like features were also predicted in the central and southern basin, as well as a transition from western intensified flow in the south to eastern intensified flow in the north during most of the year.

[6] Aiming at a better description of the circulation pattern and the hydrographic structure of the Red Sea during the poorly sampled summer period, a cruise was conducted in the Red Sea basin during the summer of 2001, and the basic findings are described in this paper. In section 2 we provide a brief description of the cruise and the data collected. In section 3 the basic characteristics of the Red Sea water masses during summer are reviewed and the hydrographic structure observed along the main axis of the Red Sea is presented. In section 4 the circulation in the northern and central Red Sea is discussed, including evidence of strong eddy features. In section 5 the three-dimensional structure of GAIW intrusion in the southern Red Sea is described, tracing it from its entrance through Bab el Mandeb to the central part of the basin. Finally, section 5 includes a summary of results and a discussion of the overall picture of the summer Red Sea circulation emerging from this study.

2. Cruise Observations

[7] In order to capture the basic characteristics of the summer Red Sea circulation and improve our understanding of the dynamics governing the region, a cruise was conducted in the Red Sea basin. The cruise was carried out aboard the R/V *Maurice Ewing* from 4 August to 19 August 2001. The shipboard scientific activities consisted of hydrographic and direct current observations in the Red Sea, accompanied by direct measurements of the atmospheric parameters. A total of 96 hydrographic (CTD) stations were occupied during the cruise. Figure 1 presents the ship track and the station locations. At each station, profiles of temperature, salinity (conductivity), and dissolved oxygen concentration were collected using a Sea-Bird-9plus CTD system. Water samples for the calibration of the salinity and dissolved oxygen were collected at about one third of these stations.

[8] Upper ocean currents were continuously measured with a 150 kHz Narrow-Band Acoustic Doppler Current Profiler mounted in the ship's transducer well (SADCP). The depth range of good velocity data typically extended to 300–400 m below the vessel, depending on sea state conditions. All the standard meteorological fields were recorded by the R/V *Maurice Ewing* weather pack. The recorded wind, projected on the main NNW-SSE axis of the Red Sea basin (which is the predominant wind component), is plotted in Figure 2 as a function of latitude. In the northern and central part of the basin the wind is northwesterly, with higher values in the northern and lower values in the central part, in agreement with the typical summer conditions [*Sofianos and Johns*, 2002]. In the southern portion of the Red Sea the winds are highly variable in magnitude and direction, and in the area of the strait southeasterly winds prevailed during the cruise, which is opposite to the climatological (NNW) wind direction.

[9] The data set acquired during the cruise was quality controlled and the results are presented in the next two sections of the paper, organized into eight transects sampled during the cruise. The first transect, presented in the next section, follows the main axis of the basin and consists of 20 stations (cyan dots in Figure 1). The remaining seven transects are marked in the map of Figure 1 by the letters A to G and presented in section 4.

3. Hydrographic and Current Structure Along the Axis of the Red Sea

3.1. Stratification and Water Masses

[10] The stratification pattern and main water masses involved in the summer Red Sea circulation are clearly depicted from the 20 stations roughly following the central axis of the basin (cyan dots in Figure 1). The potential temperature, salinity and dissolved oxygen concentration along this section are shown in Figures 3–5. The most prominent feature, characteristic of the summer circulation and exchange with the Indian Ocean, is the temperature, salinity and oxygen minimum located around a depth of

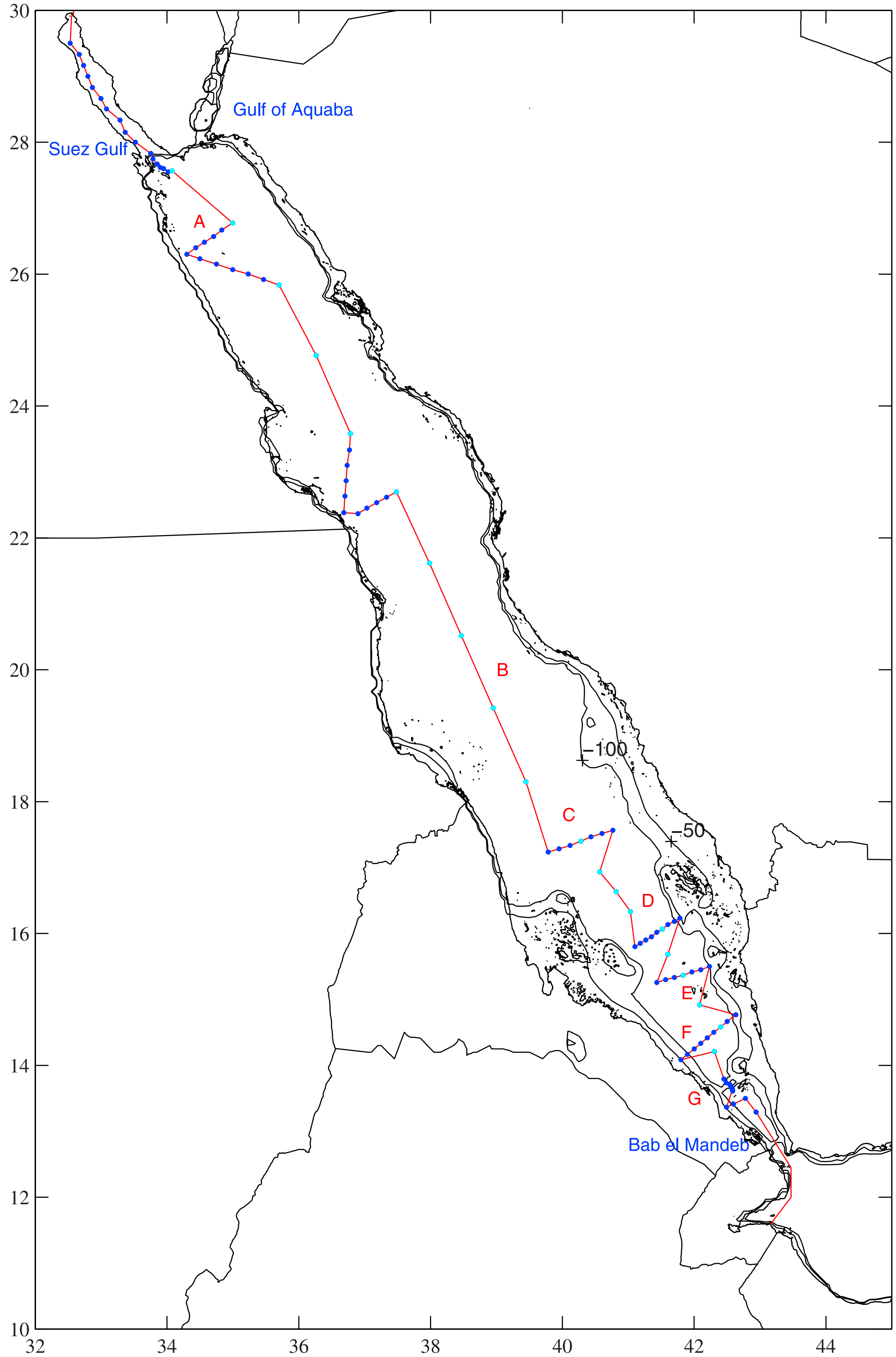

Figure 1. Location of the stations occupied during the cruise and transect (A through F) presented in the data analysis.

75 m at the southern end of the basin. It is associated with Gulf of Aden Intermediate Water (GAIW) inflowing from the Gulf of Aden during the summer season as an intruding subsurface layer. Overlying the GAIW layer is the Red Sea Surface Water (RSSW), which is warmer and saltier than the GAIW but has widely varying characteristics through the basin. Contrary to the winter situation, the RSSW is moving generally southward through the basin during summer and exiting in a thin surface layer through the Bab el Mandeb [*Murray and Johns*, 1997; *Sofianos et al.*, 2002]. Underlying the GAIW are two water masses: (1) the Red Sea Overflow Water (RSOW) formed mainly by open ocean convection in the northern Red Sea [*Sofianos and Johns*, 2003] with salinities close to 40 psu, which forms the hypersaline outflow at the bottom of the strait (much weaker than during winter but still present – *Murray and Johns*,

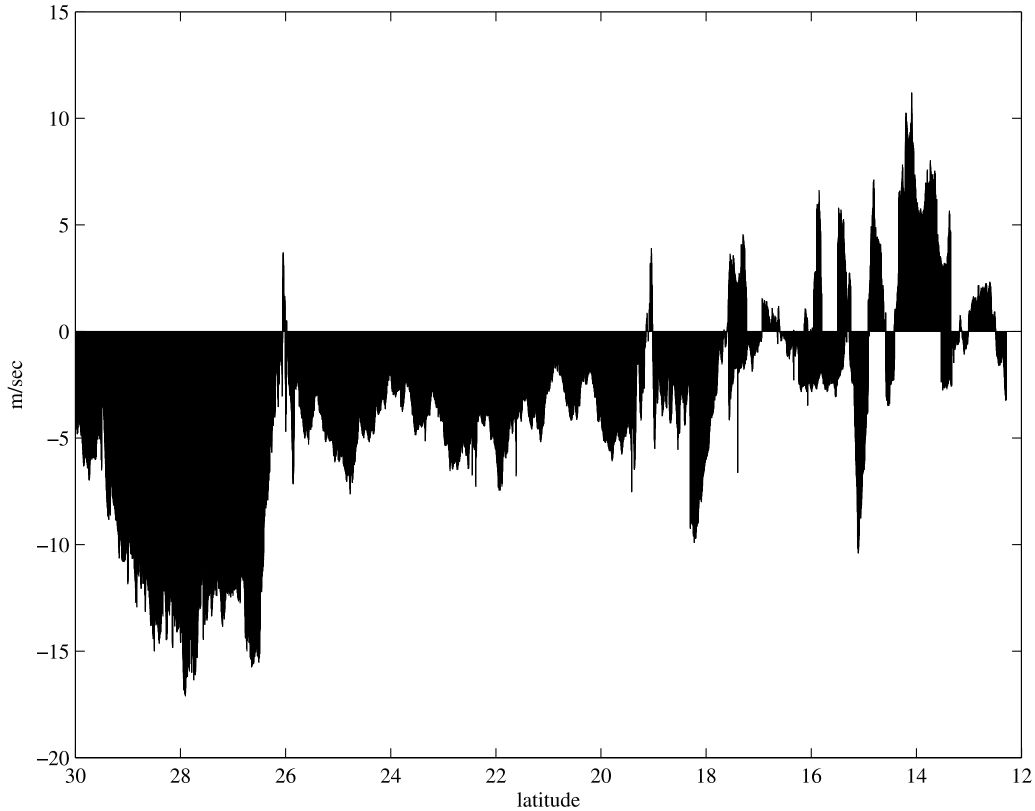

Figure 2. Along-axis winds recorded during the Red Sea cruise. Negative values correspond to northwesterly winds; positive values correspond to southeasterly winds.

1997), and (2) the Red Sea Deep Water (RSDW) which is mainly formed in the Gulf of Suez area [*Maillard*, 1974; *Wyrtki*, 1974] and fills the basin from about 200 m to the bottom. The latter has temperature/salinity characteristics very similar to the RSOW and it is distinguished mainly by its very low oxygen concentration [*Woelk and Quadfasel*, 1996]. Although the basic structure of the exchange flow is adequately described in the strait area, the place and mechanisms where the RSSW acquires its characteristics, the fate of the GAIW inside the basin, and the structure of the RSOW layer inside the basin are not well understood at present.

[11] Strong latitudinal gradients of all hydrographic characteristics are evident in the surface and GAIW layers, related to the gradients in the air-sea interaction fields and the mixing processes inside the basin. The GAIW layer characteristics are rapidly diminished as it flows to the north between the warmer, saltier, and more oxygenated RSSW and RSOW layers, and the last traces of the water mass can be found in the area near 22°N. At the southern part of the basin we can observe two oxygen minima, one centered at around 75 m depth and the second at around 400 m depth. The former is associated with the GAIW and presents minimum values below around 10 μmol/kg. The latter is related to the RSDW, and in particular to the "old" deep waters as they recirculate toward the north. As predicted by *Cember* [1988] on the basis of ^{14}C and ^{3}He concentrations, deep waters sink to the bottom levels in the northern part of the basin, follow a southward movement and reaching the shallow area close to the strait of Bab el Mandeb they are uplifted and follow a slow northward movement. Relatively high dissolved oxygen concentration is observed in the bottom waters of the northern end of the Red Sea, which can be characterized as "new deep waters" formed during the past winter. Following the slow clockwise movement the dissolved oxygen concentration of the "older waters" is depleted.

[12] Above this dissolved oxygen minimum lies the RSOW layer, which is formed during winter at the northern part of the basin [*Sofianos and Johns*, 2003] and flows to the south and out of the basin. It is characterized by relatively high dissolved oxygen concentration, which close to the Bab el Mandeb area is located at about 150 m depth. The highest values of dissolved oxygen concentration are detected in the surface and subsurface waters in the northern part of the basin. Apart from the lower biological activity in the region, as compared to the southern part of the basin, the subsurface maximum is also related to a very high salinity maximum (maximum salinity over 40.6 psu) and can be associated with relatively buoyant Gulf of Suez waters, outflowing from the Gulf during summer (S. S. Sofianos et al., manuscript in preparation, 2007).

3.2. Along-Basin Variability in Surface and Intermediate Water Properties

[13] A composite potential temperature-salinity diagram produced from the CTD observations at all stations carried out during the summer 2001 Red Sea cruise is presented in Figure 6. The structure of the T/S properties roughly follows a south to north orientation, with profiles at the left

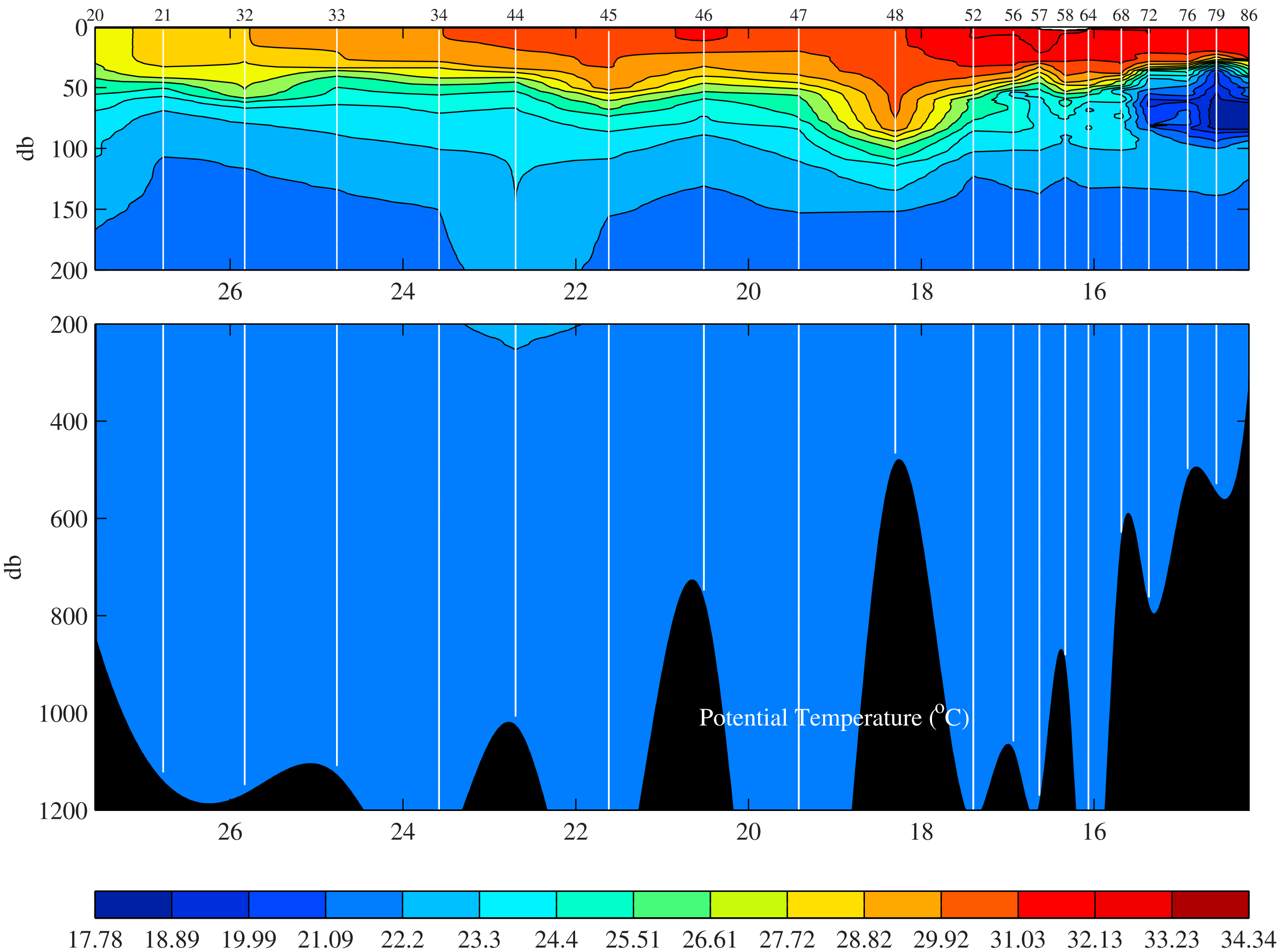

Figure 3. Potential temperature section from the 20 stations following the main axis of the Red Sea (top axis indicates the station number and bottom axis indicates latitude).

side of the diagram originating from the southern part of the basin and those on the right side originating from the north. A very distinct salinity (35.7 psu) and potential temperature (16.5°C) minimum in the lower left corner of the diagram marks the GAIW entering the Red Sea from the Bab el Mandeb. The intruding waters are mixed rapidly with the overlying (RSSW) and underling (RSOW) layers and their T/S signature is diminishing as the GAIW travels northward in the basin. At the surface the salinity of the RSSW increases from about 37.5 to 40 from the southern to northern ends of the Red Sea. The deeper layers (including RSOW and RSDW) on the other hand present fairly constant temperature and salinity characteristics along the basin.

[14] The changes in the characteristics of the GAIW are demonstrated clearly in Figure 7, where the potential temperature, salinity and oxygen at the salinity minimum, and depth of the salinity minimum, are plotted as a function of latitude. In the southern half of the basin there are strong latitudinal gradients with the potential temperature increasing from 16.5 to almost 33°C and the salinity from 35.7 to over 38 psu. At the same time, the depth of the salinity minimum gradually decreases, and while at the entrance of the basin the core of GAIW is located at a depth of around 75 m it progressively becomes very shallow. Although we cannot identify with accuracy the northern limit of the intrusion, temperature and salinity values that characterize the water mass cannot be traced north of 22°N, which can be hypothesized as the northern limit of the intrusion waters. The presence of near surface minima is not considered a signal of GAIW. Other subsurface minima in the northern part of the basin (around 26°N) are associated with high oxygen concentration, which is an indication of local sources of relatively low-salinity water. Although the strong circulation features, observed during the cruise, may disperse "pockets" of water with GAIW origin in the northern part of the basin, no clear signal was detected north of 22°N. This latitude is close to latitude predicted by *Smeed* [1997] for the northernmost intrusion latitude at the end of the summer season (end of September) from historical data. Whether the signal of GAIW is still propagating northward and beyond this limit for the rest of the summer season (from end of August to end of September) is not clear.

[15] Potential temperature and salinity trends in the surface layer (Figure 8) show that following the north-south direction potential temperature initially increases from 28°C to a maximum of 33.8°C near 17.3°N. From this latitude, a decreasing trend is observed and the surface temperature at the exit of the basin is about 31.5°C. The surface salinity presents a continuous decreasing trend to the south ranging

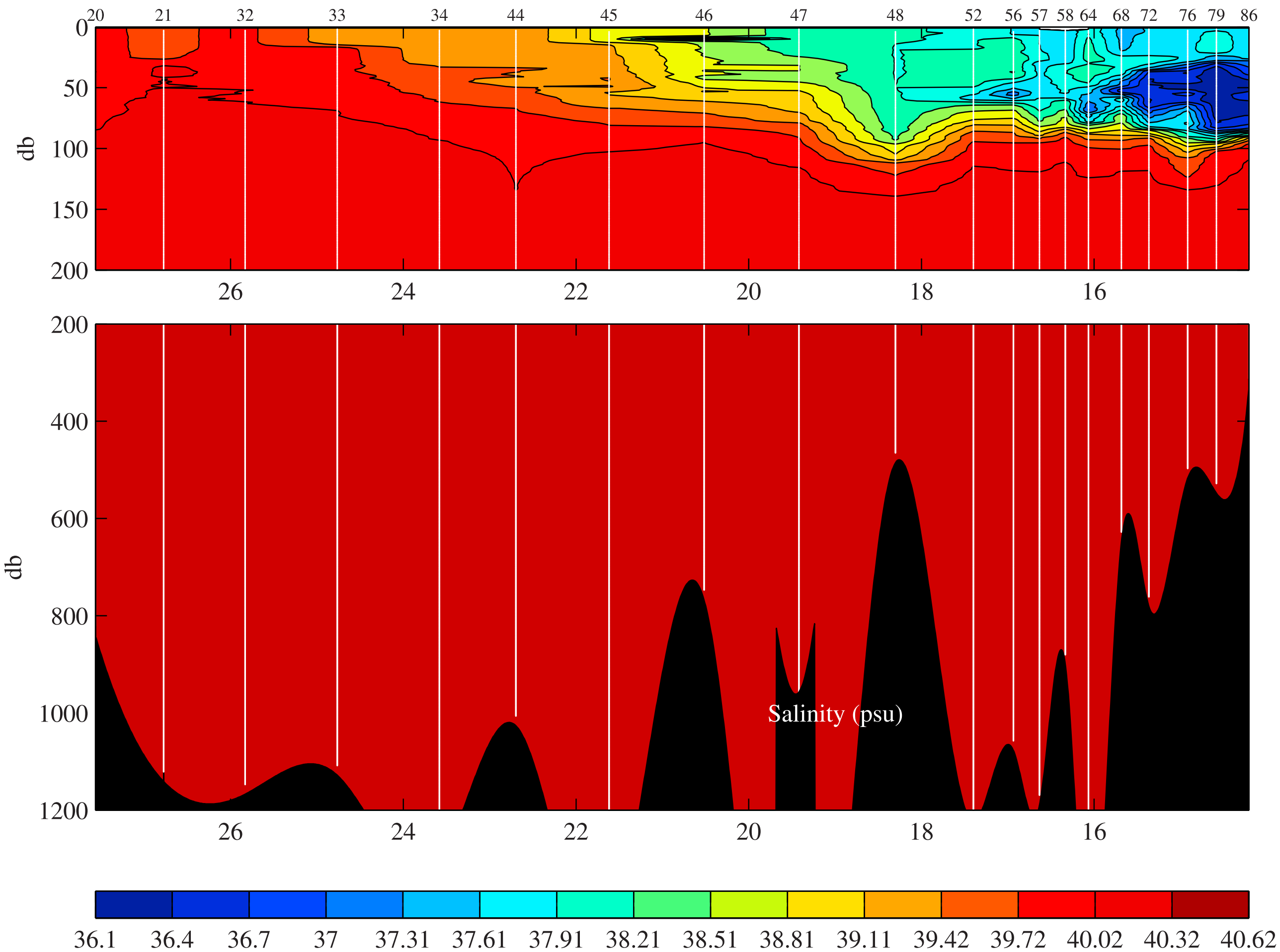

Figure 4. Salinity section from the 20 stations following the main axis of the Red Sea.

from around 40.2 psu in the northern end of the basin to 37.5 psu at the strait of Bab el Mandeb. The temperature and salinity trends in the northern and central parts of the Red Sea are consistent with the north-south trends of the air-sea heat and freshwater fluxes [*Sofianos and Johns*, 2002], which acquire their maximum losses at the northern end of the basin throughout the year. In summer the presence of these gradients is emphasized by the northerly wind field, which has its maximum value in the northern end of the basin [*Sofianos and Johns*, 2003]. During the period of the cruise, which corresponds to the middle of the summer season, northerly, relatively strong winds predominate in the northern and middle parts of the basin, while variable winds occur in the southern part. In the southern Red Sea the surface layer seems to be strongly influenced by the underlying GAIW layer, and a sharp decrease of temperature and salinity is observed. Quantification of the mixing, using the data available, is very difficult owing to the transient character of the intrusion of GAIW in the Red Sea basin. Nevertheless, the very strong trends in the water masses characteristics indicate that mixing processes are important in the region. South of 22°N, the salinity decreases abruptly and although temperature still increases until 17.5°N, the trend is then reversed until the exit of the basin (Figure 5). We can also observe these trends in the T/S diagram (Figure 6), with the southern observed values occupying the upper left corner of the diagram and the northern ones the lower right corner, so that the range in surface density becomes over 3.5 kg/m^3. Embedded in the trends, finer-scale spatial variability of the characteristics of the surface water is observed, which can be explained by the local circulation features (described in section 4), such as a temperature minimum located at 26.25°N corresponding to a strong cyclonic circulation feature.

4. Circulation in the Central and Northern Red Sea

4.1. Eddy Field in the Central Red Sea

[16] On the basis of the sparse observational data and the elongated shape of the basin, most of the descriptive and theoretical investigations of the Red Sea circulation follow a two-dimensional approach (in the latitude-depth plane) [*Neumann and McGill*, 1962; *Phillips*, 1966; *Siedler*, 1969; *Patzert*, 1974; *Tragou and Garrett*, 1997]. The circulation from these studies has the characteristics of a slow latitudinal cell, although dynamical considerations give evidence to strong mixing inside the basin [*Tragou and Garrett*, 1997; *Siddall et al.*, 2002]. Indications of a more complex and energetic three-dimensional circulation within the basin have emerged from several studies, in particular that of *Quadfasel and Baunder* [1993], which

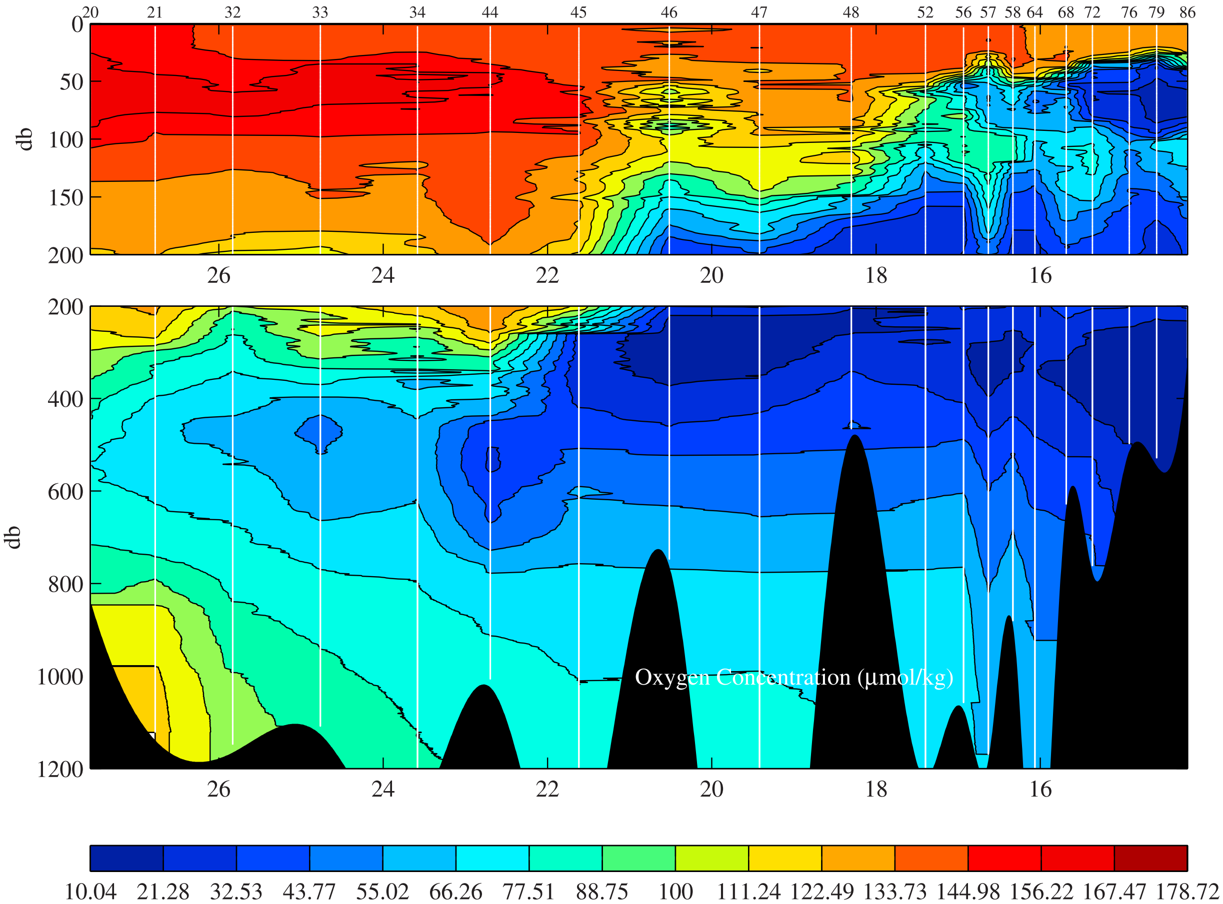

Figure 5. Dissolved oxygen concentration section from the 20 stations following the main axis of the Red Sea.

showed the presence of several quasipermanent eddies or gyres in the central part of the basin. Direct velocity measurements acquired during the cruise also reveal a fascinating three-dimensional circulation pattern which can help to explain the very rapid mixing observed in both surface and subsurface waters. Below we discuss the velocity field derived from the ship's ADCP following the cruise track with a main focus on the B transect in the central part of the basin (Figure 1).

[17] A general picture of the near surface circulation pattern during the time of the cruise can be obtained from Figure 9, where the horizontal velocity measured by the SADCP at 22 m depth is presented (this level was selected to avoid the noise recorded close to the surface layer mostly due to the ship's motion). The resulting circulation is very different from what was expected from older studies. It presents a very vigorous circulation pattern with strong variability and intense features that extend across the width of the basin. Maximum velocities exceed 1 m/s in the central sector of the Red Sea, where the most intense circulation is observed.

[18] South of 25°N a series of anticyclones were observed covering the width of the basin. The most prominent features are the three very strong anticyclones in the central part of the basin (Figure 10) between 17°N and 23.5°N. The northernmost of the three features, centered at 23°N, coincides with a permanent anticyclone described from previous observations [*Morcos*, 1970; *Morcos and Soliman*, 1974; *Quadfasel and Baunder*, 1993] and modeling studies [*Sofianos and Johns*, 2003]. It is the deepest feature detected during the cruise, penetrating to a depth of 300 m, and its maximum velocity was recorded at a depth between 100 and 150 m. The other two anticyclones, centered near 18.6°N and 21.2°N, are confined in the upper 100–150 m of the water column.

[19] The preponderance of anticyclonic features in the central Red Sea is consistent with the findings of *Quadfasel and Baunder* [1993], who developed a census of these features from available hydrographic and XBT transects of the Red Sea prior to 1987. Diagnosing the presence of anticyclones and cyclones from significant depressions or doming of isopycnals (or isotherms) in the main thermocline along the Red Sea axis, they identified 49 possible anticyclonic features and only 4 cyclonic features. Their results suggested that a permanent anticyclone was located near 23°N–24°N, and that similar but less permanent anticyclonic features were located near 20°N–21°N and 17°N–18°N. The latter feature near 18°N appears to be most pronounced in spring and summer (April–September). Thus the distribution of anticyclonic features seen in this study is consistent with expectations based on earlier studies. However, the maximum velocities observed in the present study (~1 m/s) are nearly a factor of two larger than those inferred for these features by *Quadfasel and Baunder*

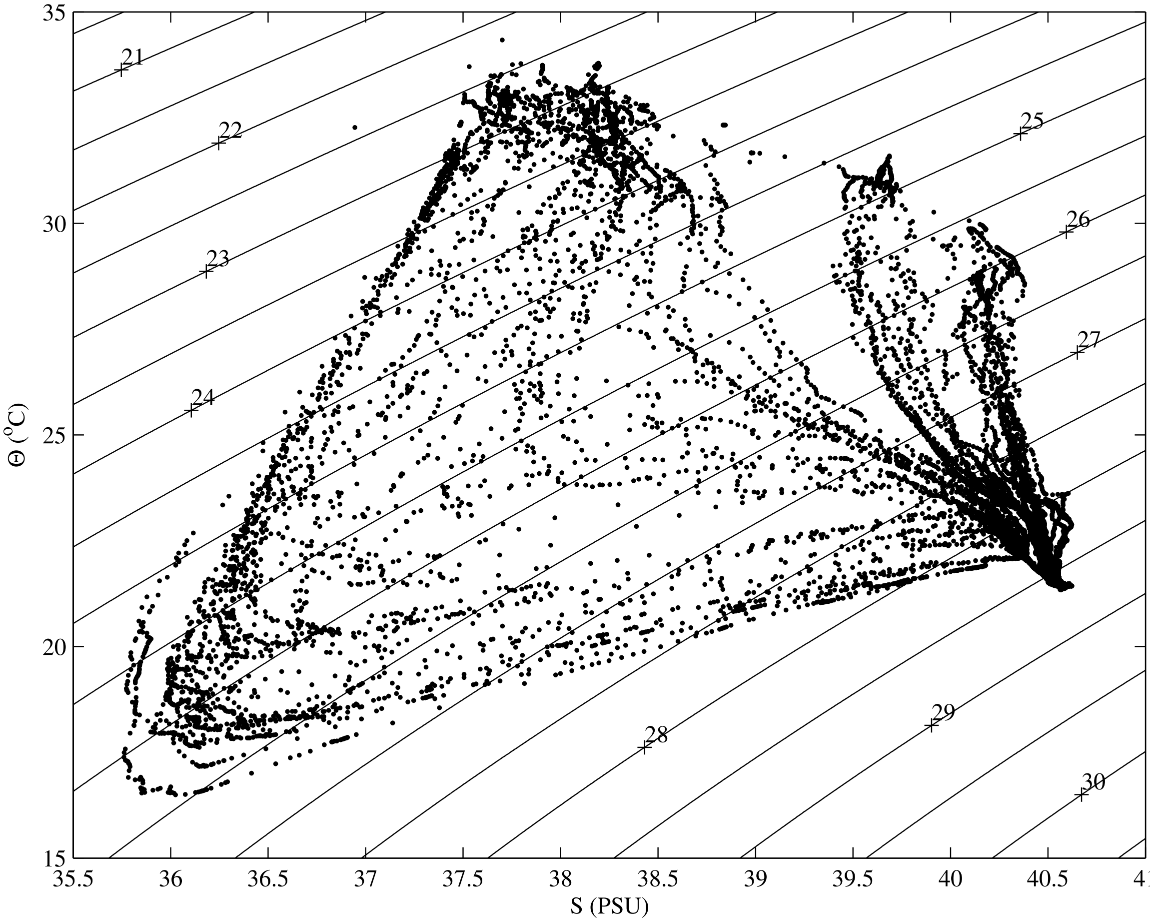

Figure 6. Potential temperature/salinity values for all stations during the Red Sea cruise, on σ_θ isolines.

[1993] from geostrophic calculations. These observations, the first to include shipboard ADCP measurements in the basin, confirm the presence of highly energetic eddy features in the central part of the Red Sea.

4.2. North Red Sea Cyclone

[20] In the northernmost part of the basin a cyclonic eddy, centered on 26°N, is observed in Figure 11, in agreement with previous observational studies in this area [*Morcos*, 1970; *Morcos and Soliman*, 1974; *Maillard*, 1974; *Clifford et al.*, 1997] and recent modeling results [*Sofianos and Johns*, 2003]. Curiously, this feature was not identified by *Quadfasel and Baunder* [1993]. Section A (Figures 11 and 12) is crossing this cyclonic gyre at about 26.5°N. Although the specific transect is not crossing the entire width of the basin, the shipboard ADCP velocity and the basic structure of the water column clearly indicate cyclonic circulation. At the western part of the section a salinity maximum is observed at the depth of 120 m, related to outflow from the Gulf of Suez (S. S. Sofianos et al., manuscript in preparation, 2007). The northward flowing part of the gyre is not fully resolved (northward velocities of a little over 20 cm/s were recorded) and is related to higher temperature and lower salinities as it carries waters that acquired their characteristics at the middle part of the Red Sea. The temperature and salinity structure of the deeper layers is also typical of a cyclone, presenting an uplifting of the denser (lower temperatures and higher salinities) isopycnals at the center of the cyclone. A very distinct dissolved oxygen concentration minimum is located at 450 m depth, related to the RSDW return flow. Maximum dissolved oxygen concentration values were recorded at 50 m depth in the whole width of the cyclonic gyre.

[21] All of the previous observational studies identifying this gyre were conducted in winter and to our knowledge this is the first clear evidence that this feature exists in summer. The available modeling studies also suggest this is a year-round feature. We therefore conclude that this is a permanent feature of the circulation, which, on the basis of the modeling studies, plays an important role in the RSOW formation processes. According to *Sofianos and Johns* [2003], a large proportion (about 65%) of the hypersaline outflow exiting the strait of Bab el Mandeb is produced in this cyclonic gyre during winter when strong buoyancy forcing provides a favorable environment for intermediate depth convection.

5. GAIW Intrusion Domain in the Southern Red Sea

[22] The southern Red Sea is also an area where few observations are available in summer, and again where most observations are only available along the axis of the basin. During the cruise, several transects (transects C to F) were

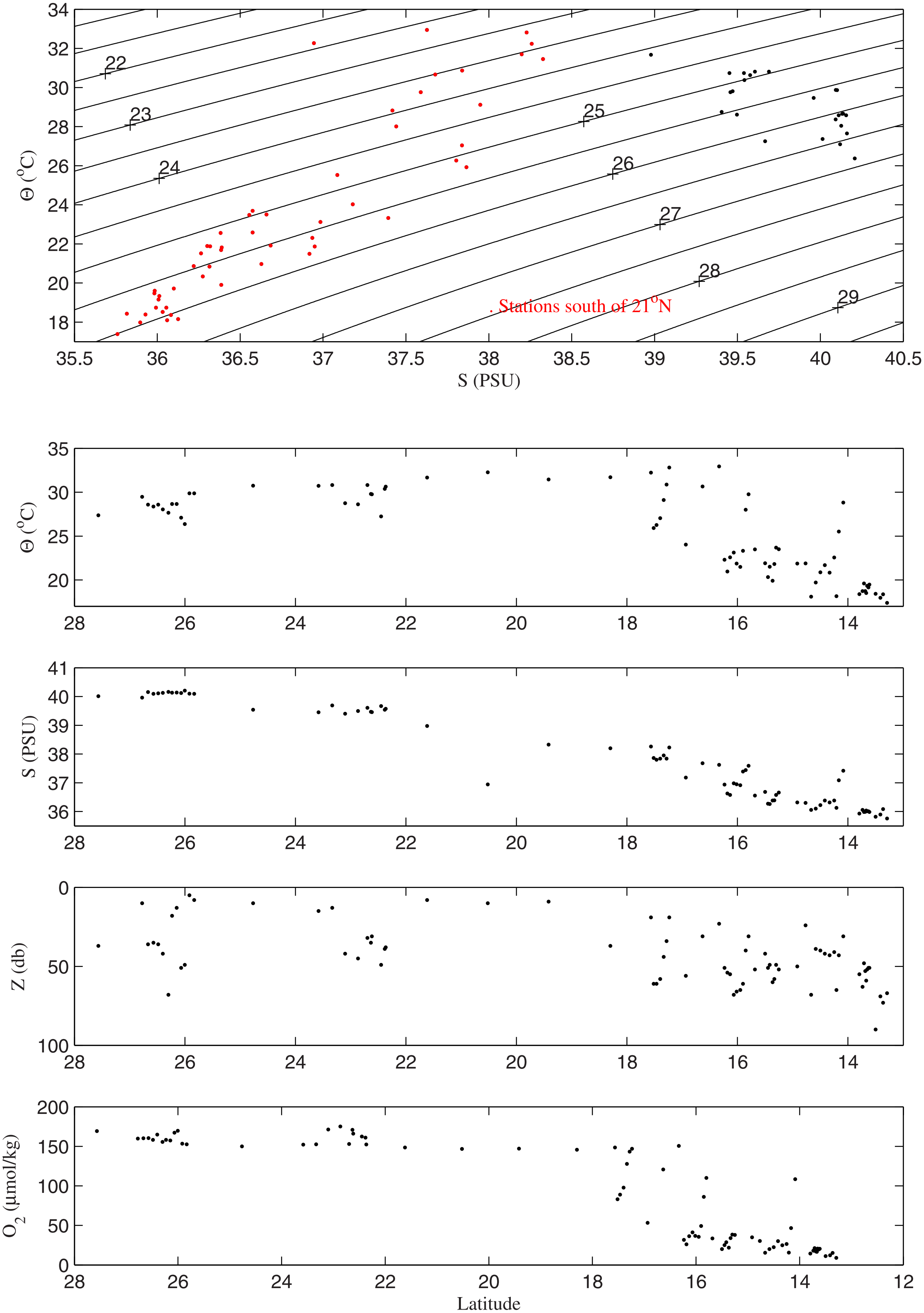

Figure 7. Potential temperature, salinity, and depth of the salinity minimum as a function of latitude.

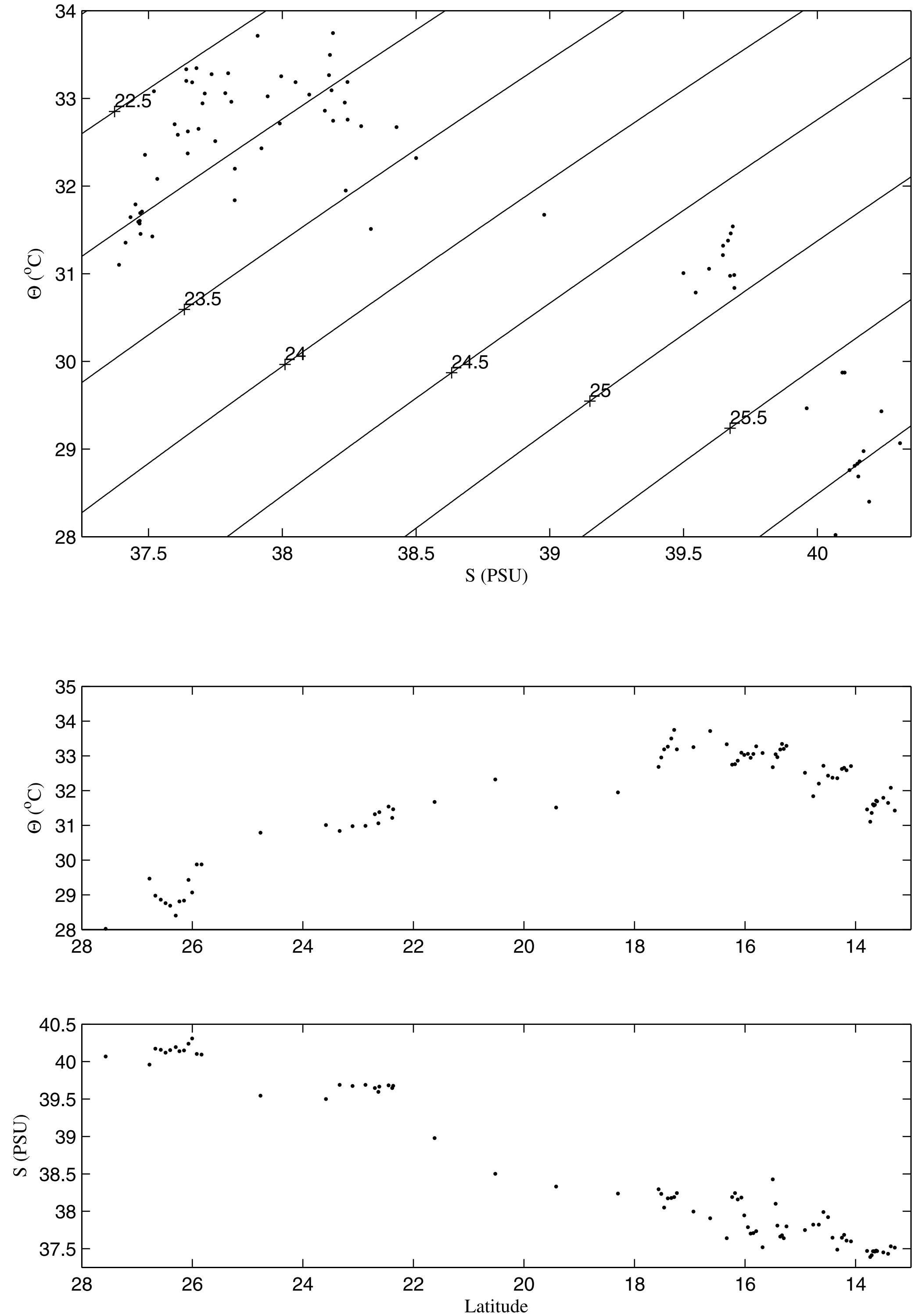

Figure 8. Potential temperature and salinity characteristics of the surface waters (upper 10 m) as a function of latitude.

made across the basin to investigate the three-dimensional structure of the GAIW intrusion, and the accompanying outflows in the surface and deeper layers. A short along-strait section (transect G) over the Hanish sill into the Bab el Mandeb was also completed. Unfortunately, the shipboard ADCP acquisition suffered intermittent failures in the latter part of the cruise, and this, coupled with increasing tidal influence in the region of the strait [*Jarosz*, 2001], render the direct velocity measurements of limited value in determining background flow patterns. Therefore we rely on the water property distributions in the sections to infer the relative flow distributions within the different layers.

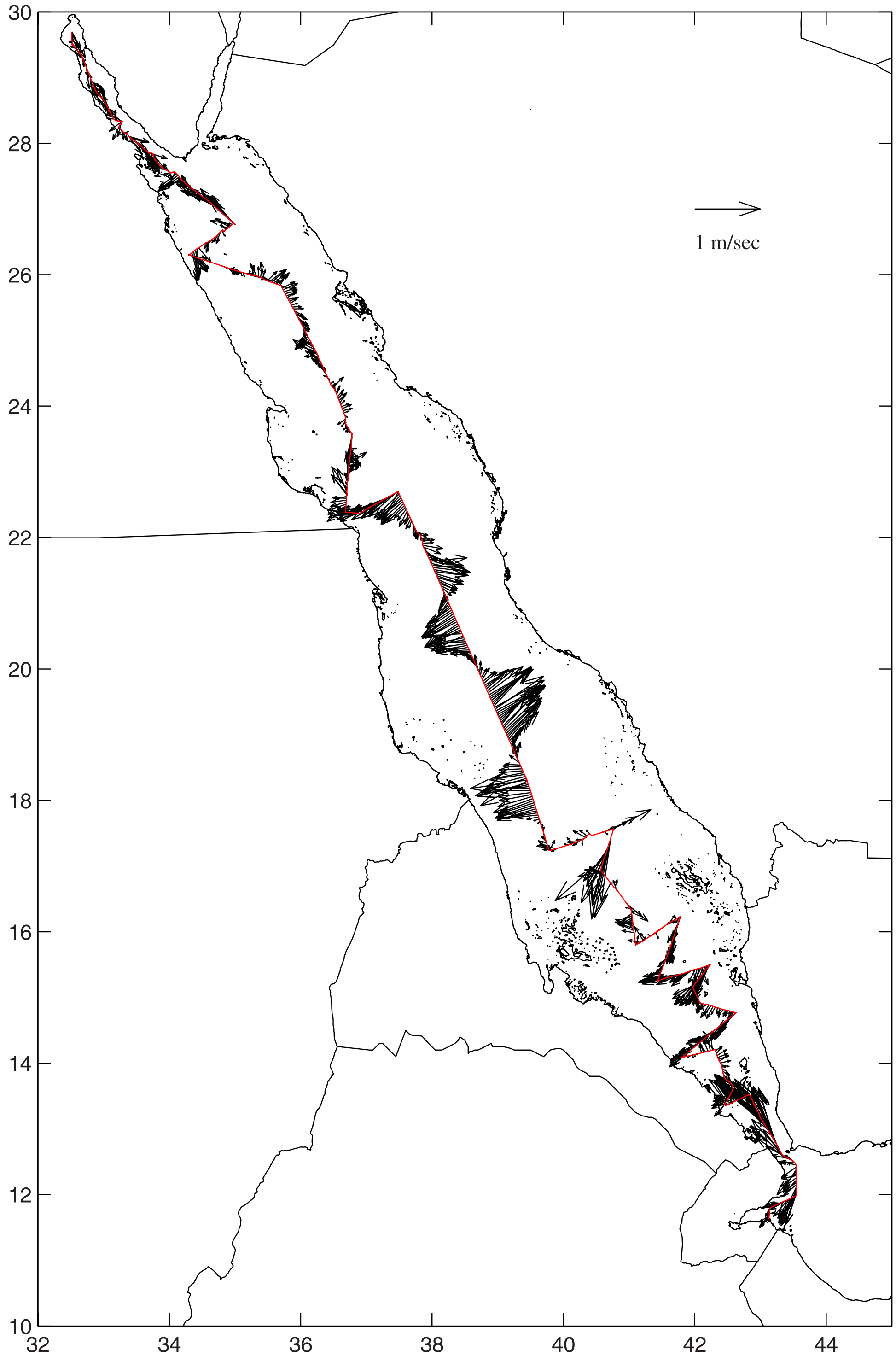

Figure 9. Horizontal velocity at the level of 22 m depth, derived from the SADCP measurements, following the track of cruise.

Elsewhere in the Red Sea, especially in the northern and central parts of the basin, tidal currents are weak [*Sultan et al.*, 1995].

[23] Transect G is located at the Hanish sill following the axis of the strait of Bab el Mandeb (Figure 13). The GAIW intrusion layer, about 50 m thick, is clearly evident at the Hanish sill. The lowest temperature and salinity values recorded at the core of the GAIW layer were 17.72°C and 35.93 psu, respectively, while its oxygen concentration is very low (14.27 μmol/kg, comparable to the value recorded at the RSDW oxygen concentration minimum). Although the cruise was carried out during the summer season, the outflow of RSOW is also strongly evident in the deeper 50 m of the water column, spilling over the sill into the

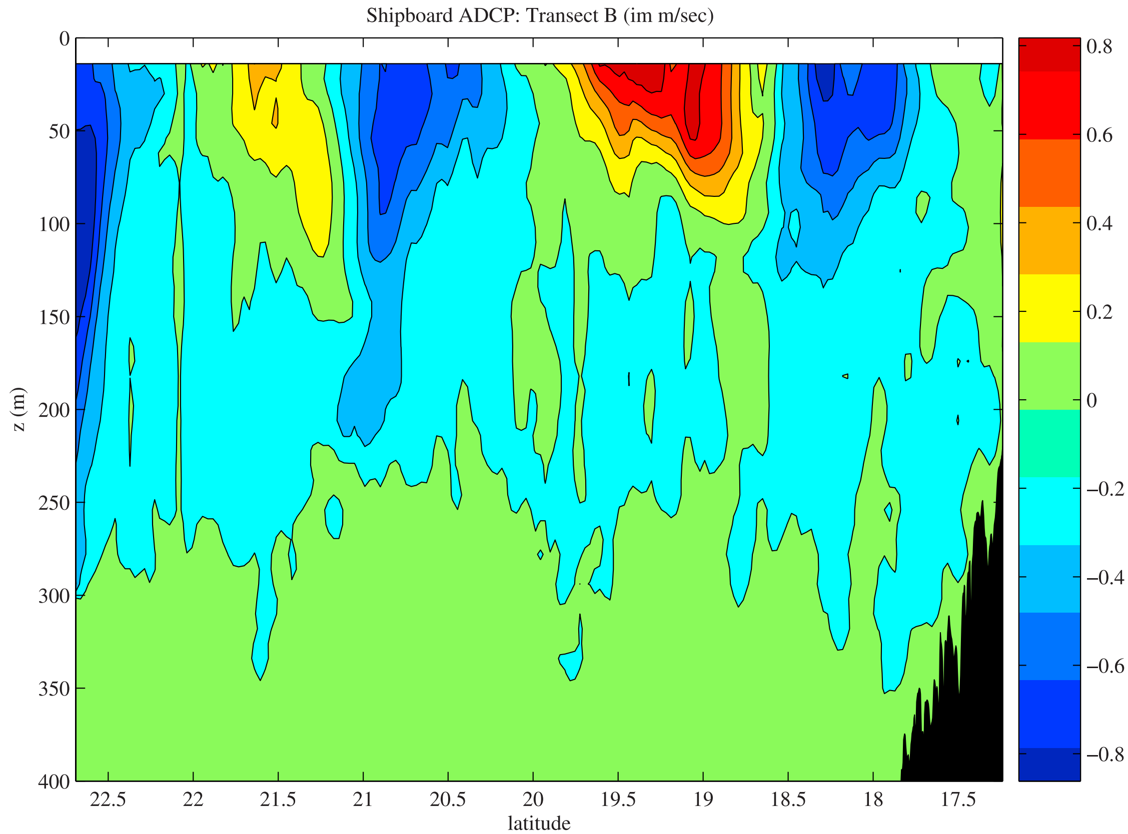

Figure 10. SADCP derived velocity at Transect B along the main axis of the basin in the central part of the Red Sea (positive values indicate eastward velocity and negative values indicate westward).

Bab el Mandeb. Compared to older summer season observations at the Hanish Sill [*Maillard and Soliman*, 1986; *Murray and Johns*, 1997; *Sofianos et al.*, 2002] the RSOW layer is significantly thicker. The presence of the RSOW in the strait region experiences strong variability at the seasonal and synoptic timescales [*Murray and Johns*, 1997; *Sofianos*, 2000]. Its temperature is about 23°C and salinity 40.5 psu. It is also clear in Figure 13 that while the lower oxygen RSDW laps up to the sill on the north side, the bulk of the deep outflow over the sill is derived from the higher oxygen RSOW that flows out above the RSDW. Overlying the GAIW is the warmer and saltier RSSW, which is generally flowing out from the Red Sea in summer. The water mass structure in the strait appears typical of the three-layer summer exchange pattern, with inward flow of the GAIW layer, and outward flow of the RSOW and RSSW layers and typical velocities of about 20–40 cm/s [*Murray and Johns*, 1997; *Sofianos et al.*, 2002].

[24] To the north, transects F and D, are located at about 16°N and 14.5°N (Figures 14 and 15) respectively. The southernmost cross-basin transect (F) is located fairly close to the Bab el Mandeb strait region. The four basic water masses involved in the summer Red Sea circulation (RSSW, GAIW, RSOW and RSDW) are clearly present in this transect. The GAIW intrusion layer is banked against the eastern (right) side of the section with about twice the thickness as at the western side, and with its core concentration values found in the eastern part of the section (18°C, 36 psu and 8.8 μmol/kg, respectively) This indicates that the GAIW flows northward into the Red Sea primarily along the eastern (Arabian) side of the basin following its entrance through the Bab el Mandeb. Conversely, the RSOW layer is banked against the western side of the section, as clearly seen in the bottom plot of Figure 14 where the highest dissolved oxygen values are found there in the 100- to 150-m depth range. The characteristics of the RSDW and its very low dissolved oxygen concentration can be identified below this level. Finally, in the surface layer, the highest salinities are found in the eastern and central parts of the section, indicating that the southward flow of RSSW from the central Red Sea is also concentrated toward the eastern coast as it approaches the Bab el Mandeb. (Section E, located approximately 130 km north of section F and 200 km from the Bab el Mandeb, shows an identical structure with the GAIW and RSSW concentrated on the eastern side of the basin and the RSOW on the west side, and is not shown.)

[25] Section D, approximately 300 km from the Bab el Mandeb (Figure 15), shows a more complicated structure in the RSOW layer but similar characteristics in the GAIW and RSSW layers. At the RSOW level, relatively high dissolved oxygen values are found on both sides of the section while a minimum occurs in the center, where the RSOW layer is thinnest and where an upward bulge of the lower oxygen RSDW can be observed. The strongest RSOW signal is still found on the western side of the section and here the RSOW

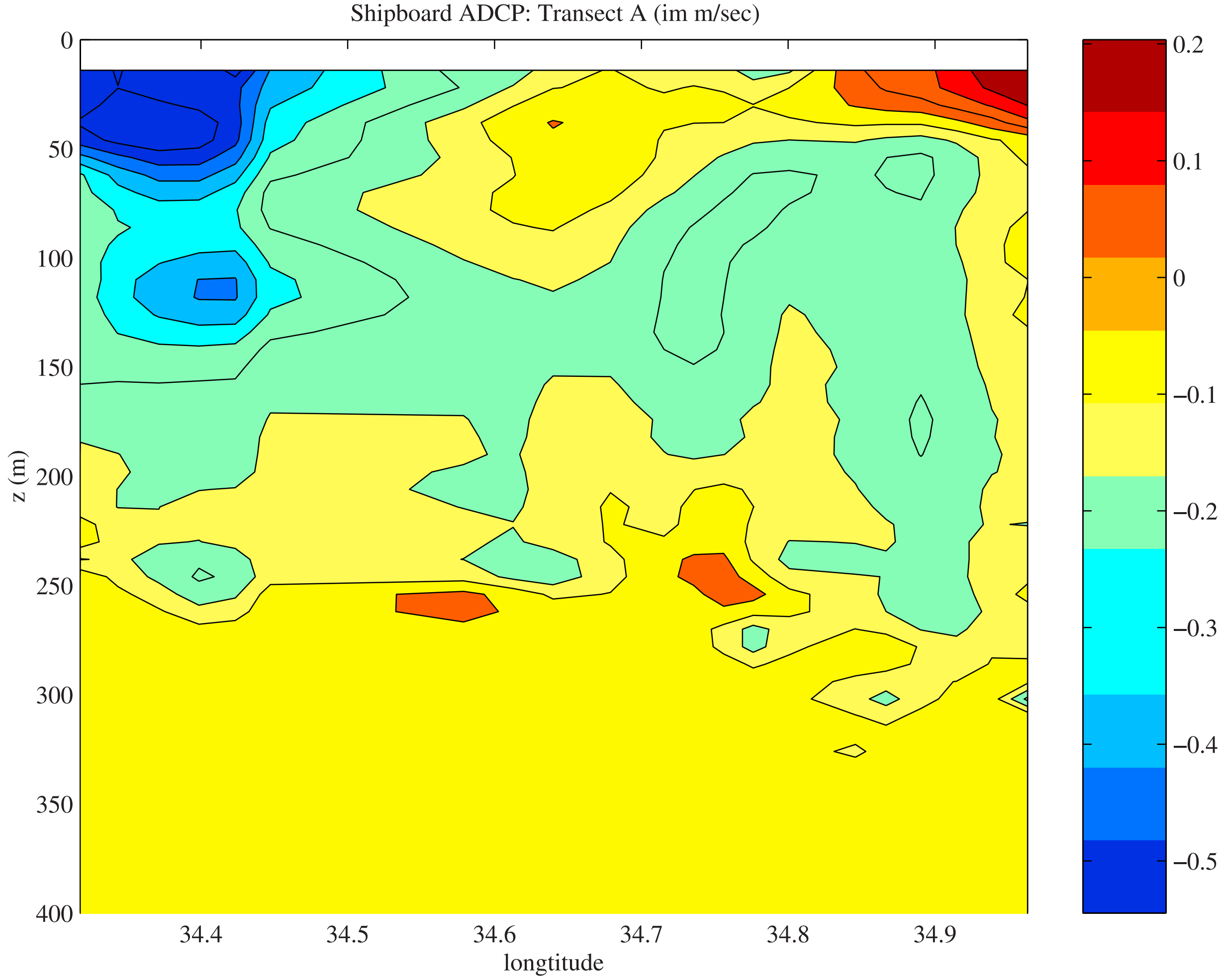

Figure 11. Shipboard ADCP velocity at transect A in the northern Red Sea.

is also the thickest. The overall pattern (including the doming of the RSDW in the basin center) is suggestive of a cyclonic recirculation of the RSOW at this location.

[26] Compared to section F (Figure 14) it can be seen that the maximum dissolved oxygen values in the RSOW layer are higher by about 10 μmol/kg, and decrease southward following the RSOW flow. This can be attributed to mixing with the GAIW and RSDW, both having very low oxygen concentrations. The overlying GAIW remains concentrated toward the eastern side of the basin, although it is now considerably thinner and covers only about half the area of the section as found at transect F. Its property extrema are also strongly diluted from those at transect F, with minimum recorded temperature, salinity and dissolved oxygen at the core of the layer at 21.5°C, 36.6 psu and 22.5 μmol/kg, respectively.

[27] In transect C, located at 17°N (Figure 16), the GAIW intrusion can be detected at 60 m depth near the eastern side of the section. At this latitude the GAIW layer is diminished to a very thin lens and its temperature and salinity characteristics are changed by the strong mixing with ambient waters, with the minimum salinity of the transect at 37.8 psu. Below that layer, dissolved oxygen distribution shows the presence of RSOW with its core between 100 and 150 m depth. The layer is thicker toward the west coast, reaching a depth of about 200 m there, however its maximum dissolved oxygen signal is displaced slightly toward the center of the basin. RSDW with very low dissolve oxygen concentration but temperature and salinity characteristics close to those of the RSOW is present below the RSOW layer.

[28] Although the GAIW intrusion domain in the southern Red Sea presents a rather complex circulation pattern, with circulation features inferred from the water mass structure, the flow pattern of the basic water masses is fairly organized. While the GAIW and surface layers are banked toward the east coast, the RSOW layer is banked toward the western coast (more evident in the southern end of the basin). During their meridional flow through the basin they present rapid changes in their characteristics.

6. Summary and Discussion

[29] The cruise data presented in this paper constitute the first intensive observational attempt to explore the three-dimensional circulation of the Red Sea. The observations were carried out during the midsummer, a period when the typical inverse-estuarine circulation characteristic of concentration basins is replaced by a three layer exchange flow at the strait of Bab el Mandeb, and when the structure in the basin is complicated by the presence of the GAIW. The

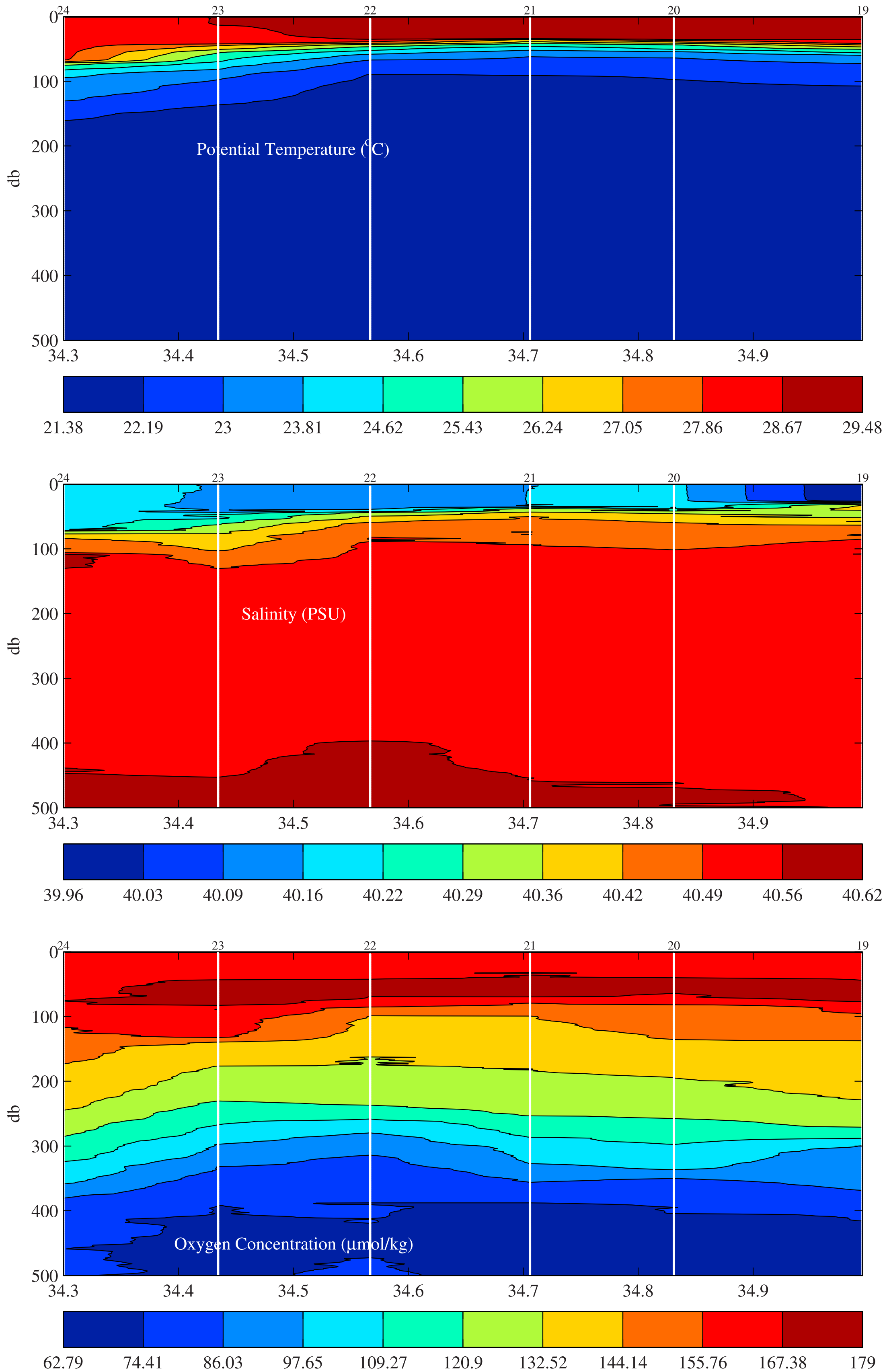

Figure 12. Potential temperature, salinity, and dissolved oxygen concentration at Transect A.

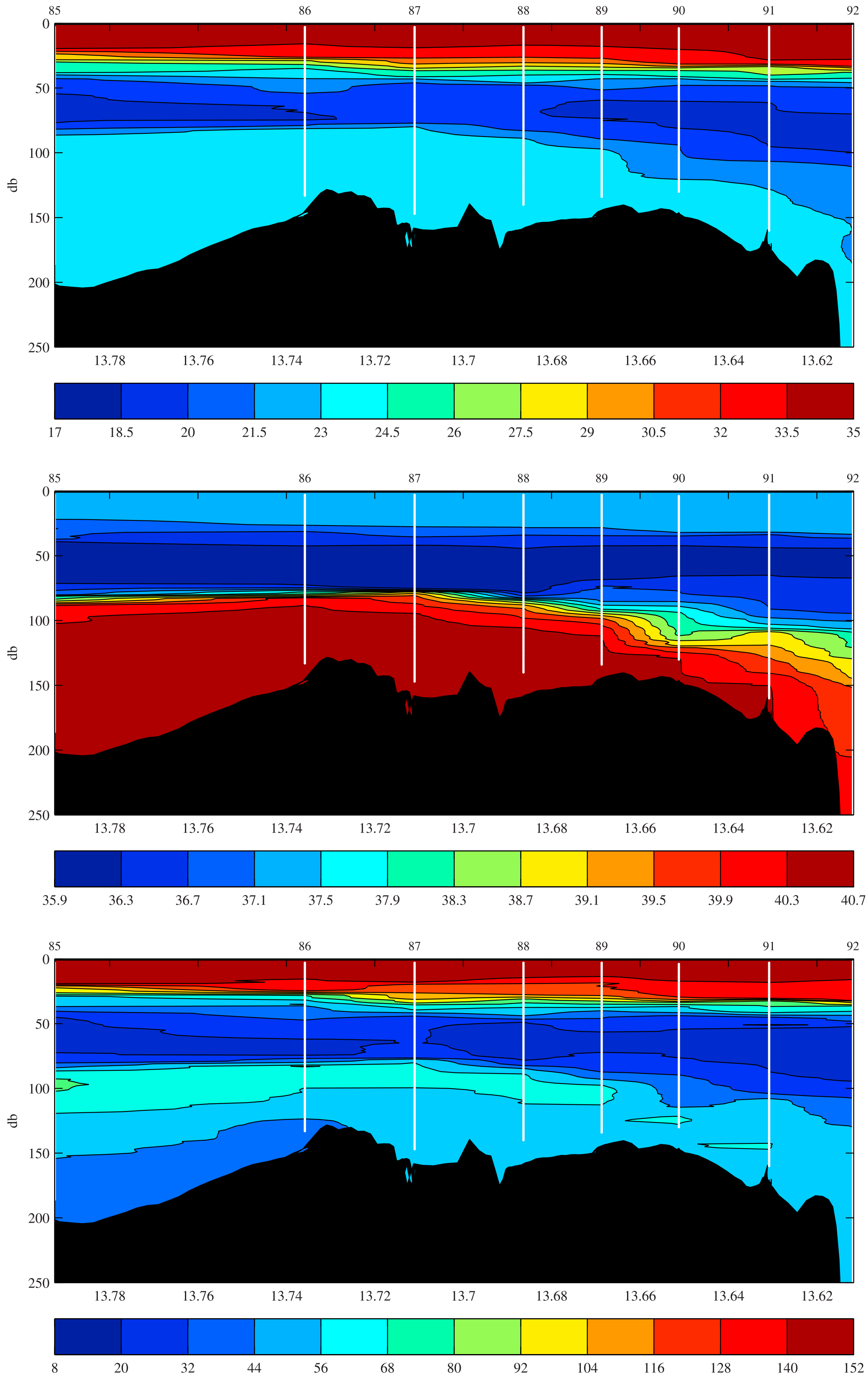

Figure 13. Potential temperature, salinity, and dissolved oxygen concentration at Hanish sill (transect G).

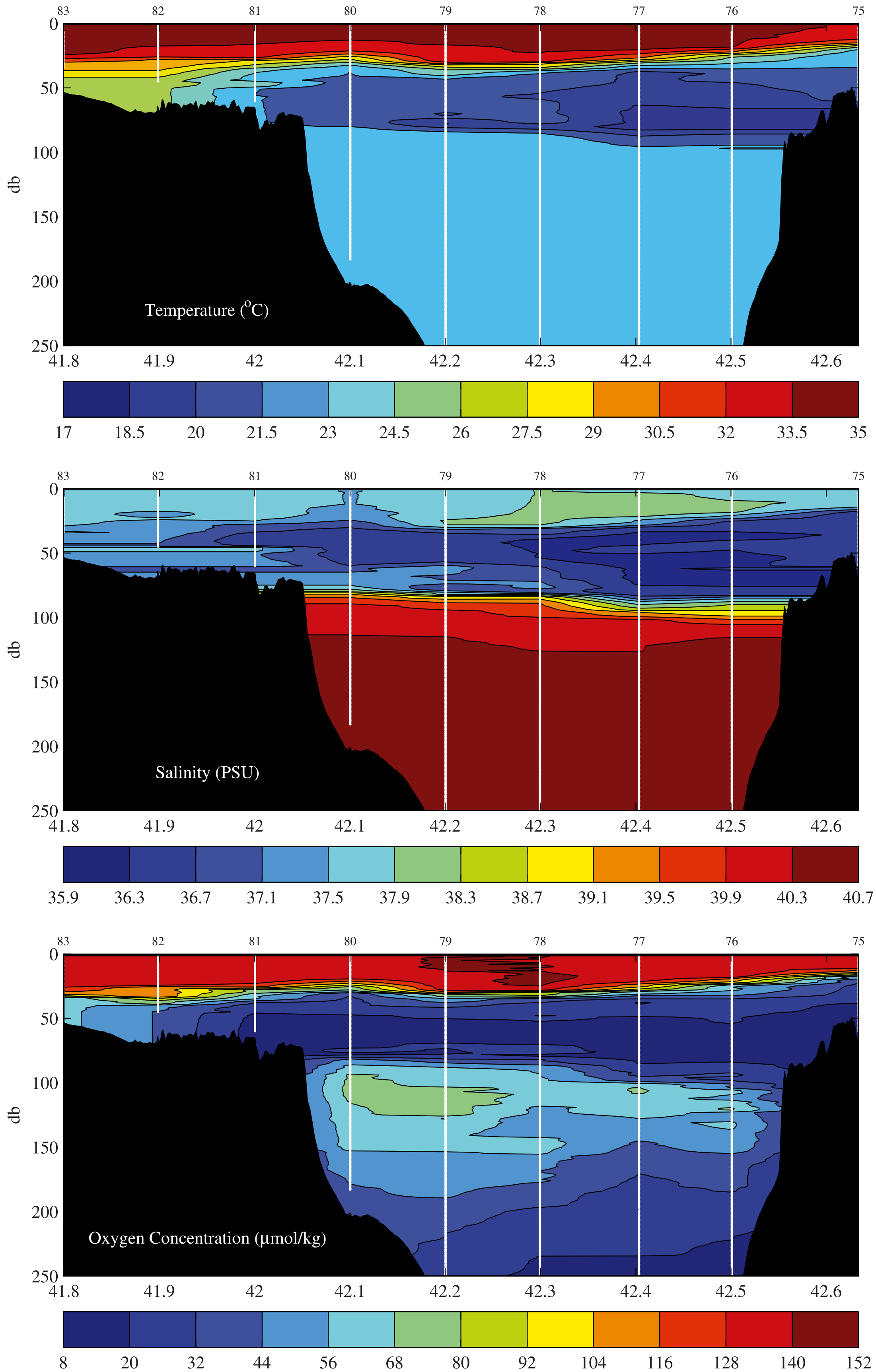

Figure 14. Potential temperature, salinity, and dissolved oxygen concentration at transect F.

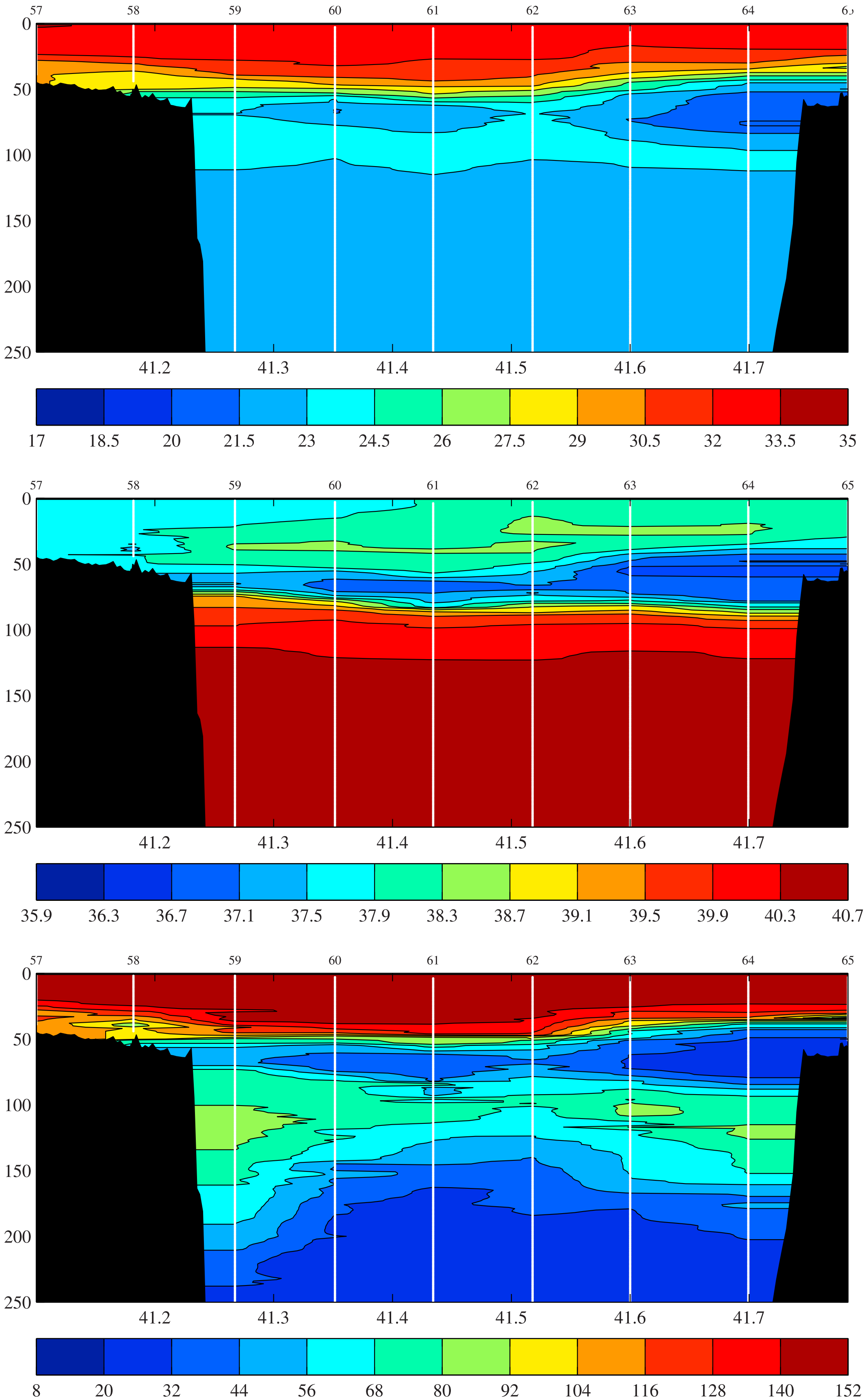

Figure 15. Potential temperature, salinity, and dissolved oxygen concentration at transect D.

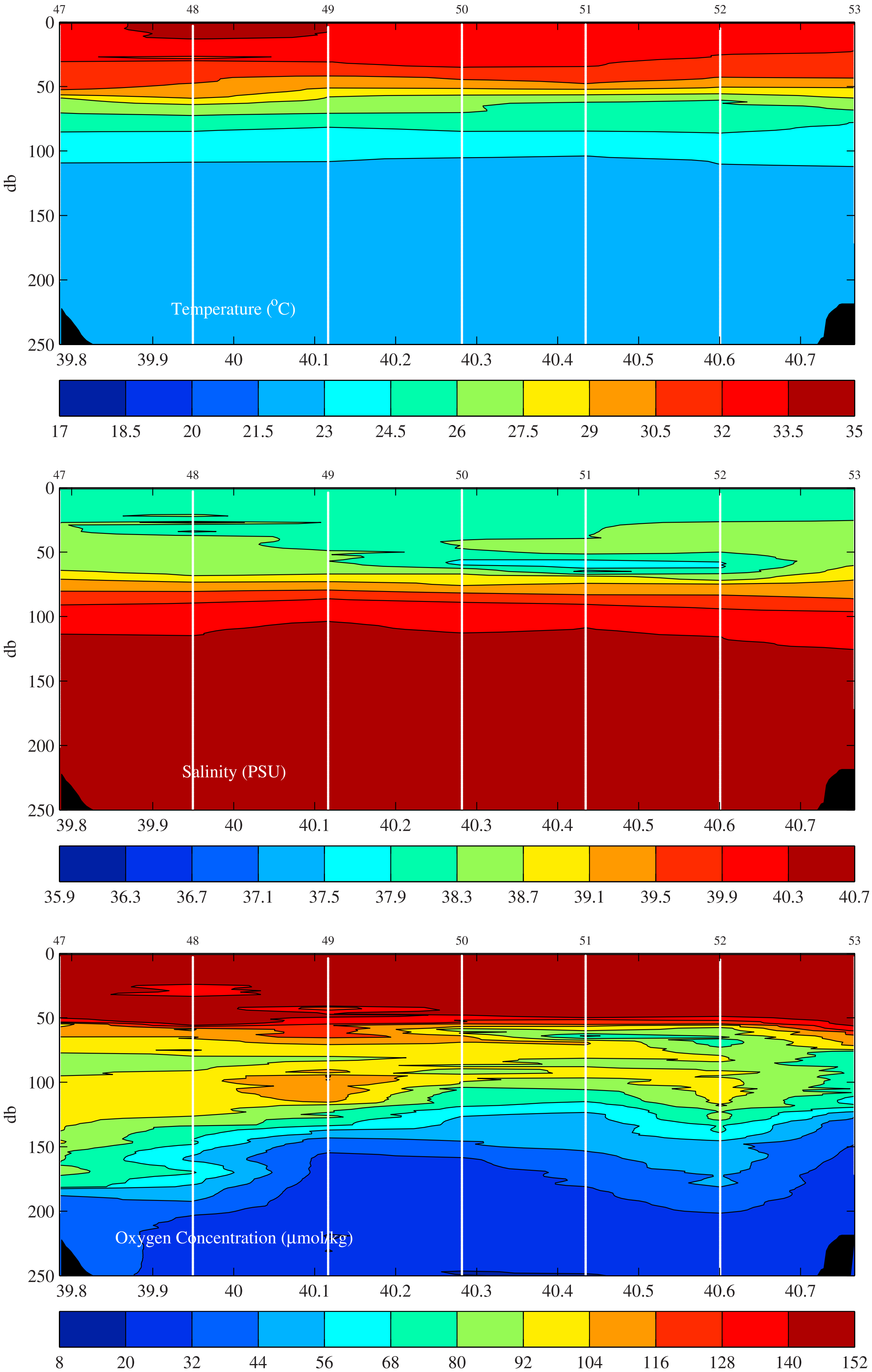

Figure 16. Potential temperature, salinity, and dissolved oxygen concentration at Transect C.

results may be subject to interannual and/or higher frequency (synoptic) timescale variability. Nevertheless, the coincidence with previous observations and modeling experiments, mostly in the two ends of the basin, indicate that features revealed during the cruise are robust and in some cases permanent characteristics of the Red Sea circulation. On the other hand, cases where the observations and models do not agree, such as the very strong features in the central basin (weaker patterns are revealed from the model results), emphasize the need for further observational efforts and improved modeling activities (both on the atmospheric forcing and the oceanic simulation techniques).

[30] During the cruise, the GAIW layer has reached a latitude that is typically identified with the northernmost limit of the intruding layer at the end of the summer season (end of September [*Smeed*, 1997]). Its temperature and salinity characteristics change rapidly with latitude (over 16°C and 2 psu in about 5 degrees of latitude) and its thickness is greatly reduced. Although GAIW and surface layer characteristics are obviously impacted by vertical mixing, we attribute these changes mainly to lateral stirring and mixing by the strong eddies in the region. In fact, consideration of the volume of GAIW entering the Red Sea (using *Murray and Johns* [1997] mean summer inflow rate of 0.22 Sv, and assuming a 50 m mean layer thickness) suggests that the GAIW would only penetrate to about 16°N by the end August if there were little or no mixing. This is where the Red Sea widens up and where the large eddies begin to take hold. Our results (Figures 4 and 7) show that this is exactly the limit to which the strong core properties of GAIW extend in the basin, after which there is rapid erosion. Therefore the propagation of the GAIW in the basin can be enhanced by the stirring action of the eddies in the basin.

[31] Both surface temperature and salinity characteristics and the surface circulation pattern show that the origin of the outflowing RSSW layer can be located in the central part of the Red Sea. South from these latitudes a southward surface flow intensified toward the eastern coast of the basin is observed. Following this pathway and affected by the surface circulation features of the southern Red Sea, the RSSW is mixed with the underlying GAIW and its characteristics rapidly change. When it reaches the area of the Bab el Mandeb strait its surface temperature is reduced to 31°C and its surface salinity to 37.5 psu.

[32] The most fascinating findings of this work are related to the circulation pattern. It is the first time that direct velocity observations are available inside the Red Sea covering the greater part of the basin. They reveal a very intense and complicated circulation pattern, which has a clear three-dimensional character in contrast to older ideas of a two-dimensional and sluggish circulation in the Red Sea. In the northern part the presence of the cyclonic gyre confirms previous observational and modeling results and shows that this is a robust and permanent feature of the Red Sea circulation. It is an important dynamical feature of the Red Sea circulation, as it is related (through modeling studies) with the production of RSOW [*Sofianos and Johns*, 2003]. *Sofianos and Johns* [2003] showed that the thermohaline forcing drives the cyclonic eddy all around the year, in contrast to the wind-driven circulation, in the northern part of the basin, which is of anticyclonic character.

[33] The central part of the Red Sea is dominated by a series of very strong anticyclones. Although further analysis and combination of different techniques may give more information on the mechanisms involved in their formation, as well as their temporal variability, it is an indication of a very strong response of the Red Sea to atmospheric forcing. Some of these features (especially the deep anticyclone located at 23°N) were resolved by previous modeling studies [*Sofianos and Johns*, 2003], but with velocities several times smaller. The underestimation of the velocity field in available modeling studies may be attributed to the climatological (monthly mean) forcing driving the model and the averaging of the fields over the period of simulation.

[34] Finally, in the southern basin the circulation is very complicated, affected by the presence of the GAIW, the complex topography of the region (with very wide continental shelves on both sides) and the higher temporal and spatial variability characterizing the atmospheric forcing of the region. The basic structure of the three-layer flow involves banking toward the coasts. The GAIW and surface layers are banked toward the east coast, and the RSOW is banked toward the western coast (more evident in the southern end of the basin) in agreement with previous observations and modeling studies. Each of these water masses undergoes strong mixing with the neighboring layers, resulting in large and systematic changes in their temperature, salinity, and (in deeper layers) dissolved oxygen characteristics throughout the southern part of the basin.

[35] **Acknowledgments.** This work was supported by Office of Naval Research under contracts N00014-95-1-0025 and N00014-03-10319. We acknowledge the excellent support provided by the Ocean Technology Group of the Rosenstiel School of Marine and Atmospheric Sciences, University of Miami, in acquiring the observations. We also thank the government and scientists from the Arab Republic of Egypt, the State of Eritrea, the Republic of Djibouti, and the Republic of Yemen for their cooperation.

References

Cember, R. P. (1988), On the sources, formation, and circulation of Red Sea Deep Water, *J. Geophys. Res.*, *93*, 8175–8191.

Clifford, M., C. Horton, J. Schmitz, and L. H. Kantha (1997), An oceanographic nowcast/forecast system for the Red Sea, *J. Geophys. Res.*, *102*, 25,101–25,122.

Jarosz, E. (2001), Tidal dynamics in the Bab el Mandeb Strait, Ph.D. thesis, 153 pp., La. State Univ., Baton Rouge.

Maillard, C. (1974), Circulation hivernale en Mer Rouge, in *L'oceanographie Physique de la Mer Rouge*, pp. 175–189, Centre National pour l'Exploitation des Océans, Paris.

Maillard, C., and G. Soliman (1986), Hydrography of the Red Sea and exchanges with the Indian Ocean in summer, *Oceanol. Acta*, *9*, 249–269.

Morcos, S. (1970), Physical and chemical oceanography of the Red Sea, *Oceanogr. Mar. Biol. Annu. Rev.*, *8*, 73–202.

Morcos, S., and G. F. Soliman (1974), Circulation and deep water formation in the Northern Red Sea in winter (based on R/V *Mabahiss* sections, January–February, 1935), in *L'oceanographie Physique de la Mer Rouge*, pp. 91–103, Centre National pour l'Exploitation des Océans, Paris.

Murray, S. P., and W. Johns (1997), Direct observations of seasonal exchange through the Bab el Mandeb strait, *Geophys. Res. Lett.*, *24*, 2557–2560.

Neumann, A. C., and D. A. McGill (1962), Circulation of the Red Sea in early summer, *Deep Sea Res.*, *8*, 223–235.

Patzert, W. C. (1974), Seasonal reversal in the Red Sea circulation, in *L'oceanographie Physique de la Mer Rouge*, pp. 55–89, Centre National pour l'Exploitation des Océans, Paris.

Phillips, O. M. (1966), On turbulent convection currents and the circulation of the Red Sea, *Deep Sea Res.*, *13*, 1149–1160.

Quadfasel, D., and H. Baunder (1993), Gyre-scale circulation cells in the Red Sea, *Oceanol. Acta*, *16*, 221–229.

Siddall, M., D. A. Smeed, S. Matthiesen, and E. J. Rohling (2002), Modelling the seasonal cycle of the exchange flow in Bab El Mandab (Red Sea), *Deep Sea Res., Part I*, *49*(9), 1551–1569.
Siedler, G. (1968), Schichtungs- und Bewegungsverhaltnisse am Sudausgang des Roten Meeres, *Meteor. Forschungsergeb. A*, *4*, 1–76.
Siedler, G. (1969), General circulation of the water masses in the Red Sea, in *Hot Brines and Recent Heavy Metal Deposits in the Red Sea*, edited by E. T. Degens and D. A. Ross, pp. 131–137, Springer, New York.
Smeed, D. (1997), Seasonal variation of the flow in the strait of Bab el Mandeb, *Oceanol. Acta*, *20*, 773–781.
Sofianos, S. S. (2000), Circulation and water mass formation in the Red Sea, and the exchange with the Indian Ocean, Ph.D. thesis, Univ. of Miami, Miami, Fla.
Sofianos, S. S., and W. E. Johns (2002), An Oceanic General Circulation Model (OGCM) investigation of the Red Sea circulation: 1. Exchange between the Red Sea and the Indian Ocean, *J. Geophys. Res.*, *107*(C11), 3196, doi:10.1029/2001JC001184.
Sofianos, S. S., and W. E. Johns (2003), An Oceanic General Circulation Model (OGCM) investigation of the Red Sea circulation: 2. Three-dimensional circulation in the Red Sea, *J. Geophys. Res.*, *108*(C3), 3066, doi:10.1029/2001JC001185.
Sofianos, S. S., W. E. Johns, and S. P. Murray (2002), Heat and freshwater budgets in the Red Sea from direct observations at Bab el Mandeb, *Deep Sea Res., Part II*, *49*, 1323–1340.
Sultan, S. A. R., F. Ahmad, and N. M. Elghribi (1995), Sea level variability in the central Red Sea, *Oceanol. Acta*, *18*, 607–615.
Thompson, E. F. (1939a), Chemical and physical investigations: The general hydrography of the Red Sea, in *John Murray Expedition 1933–34*, *Sci. Rep. 2*, pp. 83–103, Brit. Museum, London.
Thompson, E. F. (1939b), Chemical and physical investigations: The exchange of water between the Red Sea and the Gulf of Aden over the "Sill", in *John Murray Expedition 1933–34*, *Sci. Rep. 2*, pp. 105–119, Brit. Museum, London.
Tragou, E., and C. Garrett (1997), The shallow thermohaline circulation of the Red Sea, *Deep Sea Res., Part I*, *44*, 1355–1376.
Vercelli, E. (1927), Richerche di oceanografia fisica eseguite della R.N. Ammiraglio Magnaghi (1923–24), IV, La temperatura e la salinita, *Ann. Idrograf.*, *11*, 1–66.
Vercelli, E. (1931), Nuove richerche sulli correnti marine nel Mar Rosso, *Ann. Idrograf.*, *12*, 1–74.
Woelk, S., and D. Quadfasel (1996), Renewal of deep water in the Red Sea during 1982–1987, *J. Geophys. Res.*, *101*(C8), 18,155–18,165.
Wyrtki, K. (1974), On the deep circulation of the Red Sea, in *L'oceanographie Physique de la Mer Rouge*, pp. 135–163, Centre National pour l'Exploitation des Océans, Paris.

W. E. Johns, Division of Meteorology and Physical Oceanography, Rosenstiel School of Marine and Atmospheric Sciences, University of Miami, 4600 Rickenbacker Causeway, Miami, FL 33149, USA. (wjohns@rsmas.miami.edu)
S. S. Sofianos, Division of Applied Physics, University of Athens, University Campus Building PHYS-5, Athens GR-15784, Greece. (sofianos@oc.phys.uoa.gr)